

# Bumetanide derivatives AqB007 and AqB011 selectively block the Aquaporin-1 ion channel conductance and slow cancer cell migration.

Mohamad Kourghi, Jinxin V Pei, Michael L De Ieso, Gary Flynn, and  
Andrea J Yool

School of Medicine, University of Adelaide; Adelaide SA 5005 Australia (MK, JVP,  
MLDI, AJY)

Institute for Photonics and Advanced Sensing, University of Adelaide; Adelaide SA  
5005 Australia (JVP, AJY)

Spacefill Enterprises LLC; Oro Valley, Arizona 85704 USA (GF)

**Running title:** Inhibition of AQP1 ion channels

**Corresponding author:** Prof Andrea Yool; Medical School South, level 4, Frome Rd, University of Adelaide, Adelaide SA 5005 Australia

andrea.yool@adelaide.edu.au    ph: +61 8 8313 3359    fax: +61 8 8313 5384

Number of text pages: 28

Number of tables: 1

Number of figures: 6

Number of supplemental data files: 1

Numbers of words:

Abstract 246

Introduction 728

Discussion 845

*Non-standard abbreviations:* **AQP1** aquaporin-1; **AqB** aquaporin ligand  
bumetanide derivative (in numbered series)

## Abstract

Aquaporins (AQPs) in the major intrinsic family of proteins mediate fluxes of water and other small solutes across cell membranes. AQP1 is a water channel, and under permissive conditions, a nonselective cation channel gated by cGMP. In addition to mediating fluid transport, AQP1 expression facilitates rapid cell migration in cell types including colon cancers and glioblastoma. Work here defines new pharmacological derivatives of bumetanide that selectively inhibit the ion channel but not the water channel activity of AQP1. Human AQP1 was analyzed in the *Xenopus laevis* oocyte expression system by two-electrode voltage clamp and optical osmotic swelling assays. AqB011 was the most potent blocker of the AQP1 ion conductance ( $IC_{50}$  14  $\mu$ M) with no effect on water channel activity (at up to 200  $\mu$ M). The order of potency for inhibition of the ionic conductance was AqB011 > AqB007 >> AqB006  $\geq$  AqB001. Migration of human colon cancer (HT29) cells was assessed with a wound-closure assay in presence of a mitotic inhibitor. AqB011 and AqB007 significantly reduced migration rates of AQP1-positive HT29 cells without affecting viability. The order of potency for AQP1 ion channel block matched the order for inhibition of cell migration, as well as *in silico* modeling of the predicted order of energetically favored binding. Docking models suggest that AqB011 and AqB007 interact with the intracellular loop D domain, a region involved in AQP channel gating. Inhibition of AQP1 ionic conductance could be a useful adjunct therapeutic approach for reducing metastasis in cancers that upregulate AQP1 expression.

## Introduction

Osmotic water transport across biological membranes is facilitated by membrane proteins known as aquaporins (AQPs), found in all kingdoms of life (Campbell et al., 2008; Park and Saier, 1996; Reizer et al., 1993). To date, at least fifteen mammalian subfamilies have been identified, AQP0-AQP14 (Finn et al., 2014; Ishibashi, 2009). Aquaporin is organized as a tetramer of subunits, each comprising six transmembrane domains and five loops (A to E), and carrying a monomeric pore that allows the movement of water or other small solutes (Fu et al., 2000; Jung et al., 1994; Sui et al., 2001).

There is increasing recognition that certain classes of aggressive cancers depend on upregulation of AQP1 for fast migration and metastasis (Monzani et al., 2007).

Though the precise mechanism for AQP1-enhanced motility remains unknown, both ion channels and water channels are essential in the cellular migration process (Schwab et al., 2007). AQP1 expression has been linked to metastasis and invasiveness of colon cancer cells (Jiang, 2009; Yoshida et al., 2013). In mammary and melanoma cancer cells, AQP1 facilitates tumor cell migration in vitro and metastasis in vivo (Hu and Verkman, 2006). Increased levels of AQP1 expression in astrocytoma correlate with clinical grade, serving as a diagnostic indicator of poor prognoses (El Hindy et al., 2013). AQP1-facilitated cell migration in glioma cannot be substituted by AQP4, indicating more than simple water channel function is involved in the migration-enhancing mechanism (McCoy and Sontheimer, 2007).

A subset of aquaporins have been shown to have ion channel function, including AQP0, AQP1, AQP6, plant nodulin, and *Drosophila* Big Brain (Yool and Campbell, 2012). In AQP1, multiple lines of evidence have shown the cGMP-dependent



monovalent cation channel is located in the central pore at the four-fold axis of symmetry, and is pharmacologically distinct from the monomeric water pores (Anthony et al., 2000; Boassa and Yool, 2003; Saparov et al., 2001; Yu et al., 2006; Zhang et al., 2007). The AQP1 ion channel has a unitary conductance of 150 pS in physiological saline, slow activation and deactivation kinetics, and is permeable to Na<sup>+</sup>, K<sup>+</sup>, and Cs<sup>+</sup> but not divalent cations (Anthony et al., 2000; Yool et al., 1996). Loop D has been shown previously to be involved in cGMP-dependent gating of AQP1 ion channels (Yu et al., 2006). The low proportion of AQP1 water channels available to be gated as ion channels in reconstituted bilayers and heterologous expression systems has prompted uncertainty regarding the physiological relevance of the dual water and ion channel function in AQP1 (Saparov et al., 2001; Tsunoda et al., 2004). Further work has indicated that the availability of AQP1 ion channels to be activated by cGMP depends in part on tyrosine phosphorylation at the carboxyl terminal domain (Campbell et al., 2012).

Our characterization here of selective non-toxic pharmacological blockers of the AQP1 ion channel opens the first opportunity to define the functional roles of the AQP1 ion conductance. Prior to 2009, available AQP1 blockers were limited by low potency, lack of specificity, or toxicity. Mercury potently blocks AQP1 water permeability by covalent modification of a cysteine residue in loop E (Preston et al., 1993) but is highly toxic. Tetraethylammonium ion blocks the AQP1 water pore though not in all cell types (Brooks et al., 2000; Detmers et al., 2006; Sogaard and Zeuthen, 2008), and cadmium ion blocks the AQP1 ion channel (Boassa et al., 2006); but both lack selectivity for aquaporins. Effective compounds discovered recently include the arylsulfonamides AqB013 which blocks AQP1 and AQP4 water channel permeability (Migliati et al., 2009), and AqF026 which strongly potentiates AQP1

water channel activity (Yool et al., 2013). Other arylsulfonamides have been proposed as blockers of AQP4 channels (Huber et al., 2009). A distinct class of agents acting on the external side of the membrane to block human AQP1 water flux has been identified as a source of candidate lead compounds for drug development (Seeliger et al., 2013).

Work here characterizes a novel set of AqB compounds (*Aq*: aquaporin ligand; *B*: bumetanide derivative) that differentially block the AQP1 ion channel without affecting water permeability. The most potent of these, AqB011, is a promising tool for dissecting the role of the AQP1 ion channel, while sparing osmotic water permeability. Understanding functional roles and regulation of AQP1 is essential for determining the full range of physiological roles it might serve, and its possible value as a therapeutic target in cancer metastasis.

## Materials and Methods

### Oocyte preparation and injection

The use of animals in this study has been carried out in accord with the Guide for the Care and Use of Laboratory Animals, licensed under the South Australian Animal Welfare Act 1985, with protocols approved by University of Adelaide Animal Ethics Committee. Unfertilized oocytes were harvested from anesthetized *Xenopus laevis* frogs and defolliculated by incubation in Type 1A collagenase (2 mg/ml) with trypsin inhibitor (0.3 mg/ml) in OR-2 saline (82 mM NaCl, 2.5 mM KCl, 1 mM MgCl<sub>2</sub>, 5 mM HEPES; pH 7.3) at 16-18°C for 2-3 hours. Human Aquaporin-1 cDNA was provided by Prof P Agre (Preston et al., 1992; GenBank accession number NM\_198098). AQP1 subcloned into a *X. laevis*  $\beta$ -globin plasmid was linearized with BamHI and transcribed in vitro (T3 mMessage mMachine; Ambion Inc., Austin TX USA), and cRNA was resuspended in sterile water. Prepared oocytes were injected with 50 nl of water (non-AQP1-expressing control oocytes), or 50 nl of water containing 1 ng of AQP1 cRNA, and incubated for 2 or more days at 16°C in ND96 saline (96 mM NaCl, 2 mM KCl, 1 mM MgCl<sub>2</sub>, 1.8 mM CaCl<sub>2</sub>, 5 mM HEPES, pH 7.3) to allow protein expression. Successful expression was confirmed by osmotic swelling assays. Batches of AQP1-expressing oocytes which lacked robust cGMP-activated conductance responses were further incubated overnight in ND96 saline with the tyrosine phosphatase inhibitor bisperoxovanadium (100  $\mu$ M; Santa Cruz Biotechnology, Dallas TX USA) as per published methods (Campbell et al., 2012). Chemicals were purchased from Sigma-Aldrich (St. Louis MO USA) unless otherwise specified.

## **AqB compounds: synthesis and preparation**

The AqB compounds (custom-designed bumetanide derivatives) were synthesized by Dr G Flynn (Spacefill Enterprises LLC, Oro Valley AZ USA) as described in US-8,835,491-B2. To make AqB001, bumetanide was mixed with diazomethane ( $\text{CH}_2\text{N}_2$ ) generated by reaction with Diazald® to create bumetanide methyl ester (MW 344.8; ClogP 2.10), which was dissolved in hot  $\text{CHCl}_3$ , diluted with hexanes, and allowed to cool to provide the purified methyl ester as white flakes, whose mass and NMR spectra were consistent with the desired product. Reaction of bumetanide with 1.2 equivalents of 1,1'-carbonyldiimidazole (CDI) in ethyl acetate (EtOAc) under argon with heating afforded an intermediate imidazolide, which upon cooling formed a white solid that could be isolated by filtration and stored under argon for later use. Alternatively, the imidazolide solution could be reacted in situ with 2 equivalents of an amine to form the corresponding amides. In a typical reaction, the reaction mixture would be partitioned between water and ethyl acetate (EtOAc), the organic layer washed with brine, the solution filtered and concentrated, and the residue crystallized to form EtOAc/hexanes. AqB-006 (MW 413.9; ClogP 1.04) was prepared using morpholine as the amine; AqB007 (MW 470.0; ClogP 0.79) resulted from 2-(4-methylpiperazine-1-yl) ethylamine; and AqB011 (MW 434.9; ClogP 1.80) was prepared using 2-(morpholine-1-yl)ethylamine. The structures of all compounds were confirmed by high resolution mass spectrometry and NMR analysis. Chemicals were purchased from Sigma-Aldrich (St. Louis MO USA) unless otherwise specified.

Powdered compounds were dissolved in dimethyl sulfoxide (DMSO) to create 1000x stock solutions for each desired final dosage. An equal dilution of DMSO (0.1%) alone in saline was used as the vehicle control.

## **Quantitative Swelling Assay**

For double-swelling assays, each oocyte served as its own control. Swelling rates were assayed first without drug treatment (S1), then oocytes incubated for 2 h in isotonic saline with or without the AqB compounds were reassessed in a second swelling assay (S2). Swelling rates in 50% hypotonic saline (isotonic Na saline diluted with an equal volume of water) were quantified by relative increases in oocyte cross-sectional area imaged by videomicroscopy (charge-coupled device camera; Cohu, San Diego, CA) at 0.5 frames per second for 30s using NIH ImageJ software. Rates were measured as slopes of linear regression fits of relative volume as a function of time using Prism (GraphPad Software Inc., San Diego CA USA).

## **Electrophysiology**

For two-electrode voltage clamp, capillary glass electrodes (1–3 M $\Omega$ ) were filled with 1 M KCl. Recordings were done in standard Na<sup>+</sup> bath saline containing 100 mM NaCl, 2 mM KCl, 4.5 mM MgCl<sub>2</sub>, and 5 mM HEPES, pH 7.3. cGMP was applied extracellularly at a final concentration of 10-20  $\mu$ M using the membrane-permeable cGMP analog [Rp]-8-[para-chlorophenylthio]-cGMP. Ionic conductance was monitored for at least 20 min after cGMP addition to allow development of maximal plateau responses. Conductance was determined by voltage step protocols from +60 to -110mV from a holding potential of -40 mV. Recordings were made with a GeneClamp amplifier and pClamp 9.0 software (Molecular Devices, Sunnyvale CA USA).

## **Circular Wound Closure Assay**

The cancer cell lines used in this study were HT29 human colorectal

adenocarcinoma cells (Chen et al., 1987) purchased from ATCC (HTB-38; American Type Culture Collection; Manassas VA USA) which strongly express endogenous AQP1; and SW480 human colorectal adenocarcinoma cells (CCL-228; from ATCC) which express AQP5 but show little AQP1 expression. mRNA levels were evaluated by quantitative PCR and protein levels by western blot (H Dorward et al., MS in review). Confluent cultures of HT29 and SW480 cells were used in migration assays to measure effects of AqB treatments on rates of wound closure. Cells were plated in flat-bottom 96-well plates at  $1.25 \times 10^5$  cells/well in DMEM media with 10% fetal bovine serum, and incubated at 37°C and 5% CO<sub>2</sub> for 12-18 hours to allow monolayer formation. Circular wounds were created by aspirating a central circle of cells with a p10 pipette. Wells were washed 2-3 times with phosphate-buffered saline to remove cell debris. Culture media (DMEM with 2% bovine calf serum) containing either vehicle or drug treatments in the presence of a mitotic inhibitor 5-fluoro-2'-deoxyuridine (100 ng/ml) were administered into the wells. Cultures were imaged at 0 and 24 h, and analysed using ImageJ software to calculate percent wound closure by the change in area:

$$((\text{Area}_0 - \text{Area}_{24})/\text{Area}_0) \times 100$$

### **Cytotoxicity Assay**

Cell viability was quantified using the AlamarBlue cell viability assay (Molecular Probes, Eugene OR USA). Cells were plated at  $10^4$  cells/well in 96-well plates, and fluorescence signal levels were measured with a FLUOstar Optima microplate reader after 24 h incubation with concentrations of AqB011 from 1 to 80  $\mu\text{M}$ , to obtain quantitative measures of cell viability. Mercuric chloride (20  $\mu\text{M}$ ) was used as a positive control for cytotoxicity.

## **Molecular Modelling**

In silico modeling was conducted with methods reported previously (Yool et al., 2013). The crystal structure of human AQP1 was obtained from the Protein Data Bank (PDB ID: 1FQY). The tetrameric model (Supplemental Data) was generated in Pymol (Version 1.7.4 Schrödinger, LLC) using coordinates provided in the pdb file. Renderings of the AqB ligands were generated in Chemdraw (Version 13.0, PerkinElmer), then converted into pdb format using the on-line SMILES translation tool (National Cancer Institute, US Dept Health and Human Services). Both AQP1 and ligand coordinates were prepared for docking using MGLtools (Version 1.5.4, Scripps Institute, San Diego CA USA). The docking was carried using Autodock Vina (Trott and Olson, 2010) with a docking grid covering the intracellular face of tetrameric pore.

## **Data Compilation and Statistics**

Results compiled from replicate experiments are presented as box plots. The boxes represent 50% of the data, the error bars indicate the full range, and the horizontal bars are the median values. *n* values are in italics above the x-axis. Statistical differences were analyzed with one-way ANOVA and post-hoc Bonferroni tests and reported as \*\*  $p < 0.0001$ , \*  $p < 0.05$ , and not significant (NS;  $p > 0.05$ ).

## Results

### ***AQP1 ion channel inhibition by novel bumetanide derivatives***

A set of four related compounds with structural modifications at the carboxylic acid moiety of bumetanide were tested for effects on the cGMP-activated ionic conductance in AQP1-expressing oocytes. Two-electrode voltage clamp recordings of AQP1-expressing oocytes (**Figure 1**) illustrate inhibition of the ionic conductance by extracellular application of AqB007 (200  $\mu$ M) and AqB011 (20  $\mu$ M), but no appreciable block of the AQP1 ion channel with 200  $\mu$ M AqB001 or AqB006. Initial recordings before cGMP application, and responses to the first application of cGMP recordings showed typical cGMP-dependent activation, as described previously (Anthony et al., 2000). Oocytes were then transferred into saline with the indicated agents for 2 hours, during which time the ionic conductances uniformly recovered to initial levels (**Figure 2**). In response to the second application of cGMP, oocytes treated with vehicle (DMSO), AqB001 or AqB006 showed increases in conductance comparable to the first response. However, the cGMP-activated conductance responses were inhibited after treatment with AqB007 or AqB011.

Trend plots (**Fig 2A**) show that the ionic conductance in AQP1-expressing oocytes was initially low, and was activated by the first bath application of membrane permeable cGMP. The ionic conductance then recovered to basal level during a 2h incubation without cGMP, and was tested for reactivation by a second application of cGMP after treatment with vehicle or AqB compounds. Recordings for oocytes incubated in saline without DMSO during the recovery period were comparable to those for the DMSO-treated group (not shown). Non-AQP1-expressing control



oocytes showed no ionic conductance response to cGMP and no effect of the vehicle or drug treatments (**Fig 2B**).

Compiled data for the cGMP-activated ionic conductance values in AQP1-expressing oocytes are shown in the box plot (**Fig 3A**), and indicate the levels of block by 200  $\mu$ M AqB007 and 20  $\mu$ M AqB011 were statistically significant as compared with vehicle treated AQP1-expressing oocytes. Dose-response relationships (**Fig 3B**) yielded estimated  $IC_{50}$  values of 14  $\mu$ M for AqB011 and 170  $\mu$ M for AqB007.

### **AqB ion channel blockers have no effect on osmotic water permeability**

Data for oocyte volumes standardized as a percentage of initial volume at time zero illustrate the mean swelling responses over 60 seconds after introduction of the oocytes into 50% hypotonic saline (**Fig 4A**). AQP1-expressing oocytes showed consistent osmotic swelling which was unaffected by treatment with vehicle (DMSO 0.1%) or AqB compounds at 200  $\mu$ M each. Non-AQP1-expressing control oocytes showed little osmotic water permeability.

To analyze possible effects of the AqB compounds on water channel activity, a double-swelling assay was used (**Fig 4B**). After the first swelling (S1) in hypotonic saline, oocytes were incubated in isotonic saline with or without the AqB compounds (200  $\mu$ M) for 2 h before assessing the second swelling response (S2). There were no significant differences between the first and second swelling rates in any of the treatment groups, confirming that the AqB ion channel agents did not affect AQP1 osmotic water permeability.

## **Molecular modelling of candidate intracellular binding sites**

Putative binding sites on the AQP1 ion pore for AqB011 and AqB007 in the intracellular loop D domain can be suggested based on structural modelling and docking analyses (**Figure 5**). In silico modeling suggested the sites for the most favorable energies of interaction for AqB007 and AqB011 were located at the intracellular face of the central pore (**Fig 5A**). Interestingly, the model predicted hydrogen bonding between the uniquely elongated moieties of the two effective AqB ligands and the initial pairs of arginine residues in the highly conserved loop D motifs from two adjacent subunits (**Fig 5B**); the same arginines (R159 and R160 in human AQP1) have been shown to be involved in AQP1 ion channel gating but not water channel activity in prior work (Yu et al., 2006). The more compact AqB006 docked weakly at a different position in the central vestibule (not shown). While in silico modeling does not define actual binding sites, it provides a testable hypothesis for future work, and offers intriguing support for the role of loop D in modulating AQP1 ion channel gating. The most favorable energy of interaction was calculated for AqB011 (at -9.2 kcal/mol). The next most favorable energy of interaction for AqB compounds with the AQP1 channel was for AqB007 (at -7.0 kcal/mol), followed by AqB006 (at -6.0 kcal/mol). This order of interaction strength for the AqB series matched their order of efficacy for inhibition of the AQP1 ion channel conductance (Figure 3).

## **Inhibition of AQP1 ion channel activity slows cancer cell migration**

The effects of AqB006, AqB007 and AqB011 were tested in migration assays of human HT29 colon cancer cells (**Figure 6**) which natively express AQP1. Net migration rates were calculated from the percent closure of a circular wound area at

24 h (**Fig 6A**). Results showed that cancer cell migration was not impaired by AqB006, but was impaired significantly by AqB007 at 100  $\mu$ M, and AqB011 at 50  $\mu$ M and 100  $\mu$ M, as compared with vehicle-treated control HT29 cells (**Fig 6B**). AqB011 was more effective than AqB007 in blocking migration, consistent with relative efficacies of the agents as blockers of the ion channel conductance. In contrast, AqB011 at 100  $\mu$ M had no effect on the migration rate of SW480 colon cancer cells (**Fig. 6B**) which express AQP5, but not AQP1, suggesting that the inhibitory effect of AqB011 appears to be selective for AQP1.

### **AqB compounds show low cytotoxicity**

There was no significant difference in viability between vehicle-treated and untreated cells, and no effect of treatment with AqB011 for HT29 cells (**Table 1**). Cell viability was assessed with alamarBlue assays. The persistence of the fluorescent signal at 24 h confirmed there was no appreciable cytotoxic effect of AqB011 treatment on HT29 cells at concentrations up to 80  $\mu$ M. Mercuric chloride as a positive control caused significant cell death, measured as a decrease in fluorescence. AqB011 at doses used to block the AQP1 ionic conductance and cancer cell migration did not impact cell viability.

## Discussion

The aim of this study was to search for selective small-molecule pharmacological agents capable of blocking the cGMP-activated cationic conductance in AQP1. Discovery of pharmacological modulators for AQP1 channels has been an important goal in the aquaporin field. AQP1 antagonist and agonist agents are expected to be useful for defining the complex roles of aquaporins in fundamental biological processes, as well as for characterizing AQP1 modulators as potential clinical agents in various conditions, such as cancer metastasis (Yool et al., 2009). AQP1 expression is upregulated in subtypes of aggressive cancer cells in which it facilitates cancer migration. Results here show that selective blockers of the AQP1 ion channel slow migration of human colon cancer cells in culture. Pharmacological inhibition of AQP1 is predicted to have a protective effect in reducing metastasis in cancer, but remains to be demonstrated in vivo.

Using bumetanide as a starting scaffold, we created an array of novel synthetic derivatives. Based on pilot data indicating a small inhibitory effect of AqB050 on the AQP1 ion channel at high doses (unpublished observations), we investigated a series of structurally related derivatives AqB006, AqB007, and AqB011, as well as a simple methylated version of bumetanide AqB001, to test for possible inhibitors of the AQP1 ionic conductance. Our findings demonstrated that AqB007 and AqB011 are effective inhibitors of the central ion pore of AQP1, with estimated  $IC_{50}$  values of 170 and 14  $\mu$ M, respectively. Both AqB007 and AqB011 showed dose-dependent inhibition of the central ion pore, whereas the intrasubunit water pores were unaffected, enabling the first dissection of physiological roles of the distinct channel functions. Measuring fluorescence signal intensity with the alumarBlue cell viability

assay showed that AqB011 was not cytotoxic at doses that produced maximal ion channel inhibition.

The inhibition by AqB011 of AQP1 ionic conductance was consistent with molecular docking studies suggesting the site of interaction is at the intracellular face of the central pore. Results revealed that AqB011 is the most energetically favored compound followed by AqB007. The predicted interaction site of AqB011 and AqB007 with AQP1 is at the loop D domain. Differences in the structures and efficacies of AqB006, AqB007 and AqB011 indicate that the structure-activity relationship of ion channel inhibition is sensitive to specific chemical modifications at the carboxylic acid position of bumetanide. The length and structure of the modification appears to be critical, and appears based on *in silico* modeling to be the region that interacts with the AQP1 channel gating loop D domain. The absence of cytotoxic effects of AqB011 at doses sufficient to block the AQP1 ion channel activity indicates that the inhibition of migration is not due indirectly to cell death. The observation that AqB011 inhibited migration in AQP1-expressing HT29 colon cancer cells, but had no effect on the migration of AQP-5 expressing SW480 colon cancer cells provides support for the idea that AqB011 is selective for AQP1. The inhibition of migration seen with AqB011 is unlikely to result from off-target effects on general metabolic function, cytoskeletal organization, actin polymerization, or signaling pathways involved in cell motility, since SW480 cell migration remained unaffected by the presence of AqB011.

AQP1 is present in barrier epithelia involved in fluid movement in the body, including proximal tubule and choroid plexus (Agre et al., 1993). It is also expressed in peripheral microvasculature, dorsal root ganglion cells, eye ciliary epithelium and trabecular meshwork, heart ventricle, and other regions in which a direct role for

osmotic water flux is less evident (Yool, 2007). Additional roles suggested for AQP1 include angiogenesis (Nicchia et al., 2013); signal transduction (Oshio et al., 2006); increased mechanical compliance to changes in pressure (Baetz et al., 2009); axonal regeneration of spinal nerves (Zhang and Verkman, 2015); recovery from injury (Hara-Chikuma and Verkman, 2006); and exocytosis (Arnaoutova et al., 2008). Relative contributions of the ion and the water channel functions in these diverse processes remain to be defined.

A possible role for the AQP1 ionic conductance (potentially in combination with water fluxes) in the control of cell volume associated with migration was supported by the results of the wound closure assays with AQP1-expressing HT29 cells. Cell migration was significantly impaired by AqB011 and AqB007, but not by AqB006. The greatest efficacy of migration block was seen with administration of AqB011. The comparable orders of efficacy for block of AQP1 ion channels in the oocyte expression system, and for block of cell migration in HT29 cultures, support the idea that the AqB011 effect on migration is mediated by block of the AQP1 ion channels directly. These data provide evidence that the ion channel activity of AQP1 has physiological relevance. Further work is needed to evaluate effects of blocking both water and ion channel activities of AQP1 together in migrating cells.

AqB011 is a new research tool for probing the physiological role of the AQP1 ion channel function in biological systems. This compound holds future promise as a possible adjunct clinical intervention in cancer metastasis. Exciting opportunities are likely to emerge from continuing discovery of pharmacological modulators for aquaporins for new treatments in cancers and other diseases.

## **Authorship Contributions**

Participated in research design: Kourghi, Pei, De Ieso, Yool

Conducted experiments: Kourghi, Pei, De Ieso

Contributed new reagents or analytic tools: Flynn

Performed data analysis: Kourghi, Pei, De Ieso, Yool

Wrote or contributed to the writing of the manuscript: Kourghi, Pei, Flynn, Yool

## References

- Agre P, Preston GM, Smith BL, Jung JS, Raina S, Moon C, Guggino WB and Nielsen S (1993) Aquaporin CHIP: the archetypal molecular water channel. *Am J Physiol* **265**(4 Pt 2):F463-476.
- Anthony TL, Brooks HL, Boassa D, Leonov S, Yanochko GM, Regan JW and Yool AJ (2000) Cloned human aquaporin-1 is a cyclic GMP-gated ion channel. *Mol Pharmacol* **57**(3):576-588.
- Arnautova I, Cawley NX, Patel N, Kim T, Rathod T and Loh YP (2008) Aquaporin 1 is important for maintaining secretory granule biogenesis in endocrine cells. *Molecular endocrinology* **22**(8):1924-1934.
- Baetz NW, Hoffman EA, Yool AJ and Stamer WD (2009) Role of aquaporin-1 in trabecular meshwork cell homeostasis during mechanical strain. *Experimental eye research* **89**(1):95-100.
- Boassa D, Stamer WD and Yool AJ (2006) Ion channel function of aquaporin-1 natively expressed in choroid plexus. *J Neurosci* **26**(30):7811-7819.
- Boassa D and Yool AJ (2003) Single amino acids in the carboxyl terminal domain of aquaporin-1 contribute to cGMP-dependent ion channel activation. *BMC Physiol* **3**:12.
- Brooks HL, Regan JW and Yool AJ (2000) Inhibition of aquaporin-1 water permeability by tetraethylammonium: involvement of the loop E pore region. *Mol Pharmacol* **57**(5):1021-1026.
- Campbell EM, Ball A, Hoppler S and Bowman AS (2008) Invertebrate aquaporins: a review. *J Comp Physiol B* **178**(8):935-955.
- Campbell EM, Birdsell DN and Yool AJ (2012) The activity of human aquaporin 1 as a cGMP-gated cation channel is regulated by tyrosine phosphorylation in the carboxyl-terminal domain. *Mol Pharmacol* **81**(1):97-105.
- Chen TR, Drabkowski D, Hay RJ, Macy M and Peterson W, Jr. (1987) WiDr is a derivative of another colon adenocarcinoma cell line, HT-29. *Cancer Genet Cytogenet* **27**(1):125-134.



- Detmers FJ, de Groot BL, Muller EM, Hinton A, Konings IB, Sze M, Flitsch SL, Grubmuller H and Deen PM (2006) Quaternary ammonium compounds as water channel blockers. Specificity, potency, and site of action. *J Biol Chem* **281**(20):14207-14214.
- El Hindy N, Bankfalvi A, Herring A, Adamzik M, Lambertz N, Zhu Y, Siffert W, Sure U and Sandalcioglu IE (2013) Correlation of aquaporin-1 water channel protein expression with tumor angiogenesis in human astrocytoma. *Anticancer research* **33**(2):609-613.
- Finn RN, Chauvigne F, Hlidberg JB, Cutler CP and Cerda J (2014) The lineage-specific evolution of aquaporin gene clusters facilitated tetrapod terrestrial adaptation. *PLoS One* **9**(11):e113686.
- Fu D, Libson A, Miercke LJ, Weitzman C, Nollert P, Krucinski J and Stroud RM (2000) Structure of a glycerol-conducting channel and the basis for its selectivity. *Science* **290**(5491):481-486.
- Hara-Chikuma M and Verkman AS (2006) Aquaporin-1 facilitates epithelial cell migration in kidney proximal tubule. *Journal of the American Society of Nephrology : JASN* **17**(1):39-45.
- Hu J and Verkman AS (2006) Increased migration and metastatic potential of tumor cells expressing aquaporin water channels. *FASEB journal : official publication of the Federation of American Societies for Experimental Biology* **20**(11):1892-1894.
- Huber VJ, Tsujita M and Nakada T (2009) Identification of aquaporin 4 inhibitors using in vitro and in silico methods. *Bioorg Med Chem* **17**(1):411-417.
- Ishibashi K (2009) New members of mammalian aquaporins: AQP10-AQP12. *Handb Exp Pharmacol*(190):251-262.
- Jiang Y (2009) Aquaporin-1 activity of plasma membrane affects HT20 colon cancer cell migration. *IUBMB Life* **61**(10):1001-1009.
- Jung JS, Bhat RV, Preston GM, Guggino WB, Baraban JM and Agre P (1994) Molecular characterization of an aquaporin cDNA from brain: candidate osmoreceptor and regulator of water balance. *Proceedings of the National Academy of Sciences of the United States of America* **91**(26):13052-13056.

- McCoy E and Sontheimer H (2007) Expression and function of water channels (aquaporins) in migrating malignant astrocytes. *Glia* **55**(10):1034-1043.
- Migliati E, Meurice N, DuBois P, Fang JS, Somasekharan S, Beckett E, Flynn G and Yool AJ (2009) Inhibition of aquaporin-1 and aquaporin-4 water permeability by a derivative of the loop diuretic bumetanide acting at an internal pore-occluding binding site. *Molecular pharmacology* **76**(1):105-112.
- Monzani E, Shtil AA and La Porta CA (2007) The water channels, new druggable targets to combat cancer cell survival, invasiveness and metastasis. *Curr Drug Targets* **8**(10):1132-1137.
- Nicchia GP, Stigliano C, Sparaneo A, Rossi A, Frigeri A and Svelto M (2013) Inhibition of aquaporin-1 dependent angiogenesis impairs tumour growth in a mouse model of melanoma. *J Mol Med (Berl)* **91**(5):613-623.
- Oshio K, Watanabe H, Yan D, Verkman AS and Manley GT (2006) Impaired pain sensation in mice lacking Aquaporin-1 water channels. *Biochemical and biophysical research communications* **341**(4):1022-1028.
- Park JH and Saier MH, Jr. (1996) Phylogenetic characterization of the MIP family of transmembrane channel proteins. *J Membr Biol* **153**(3):171-180.
- Preston GM, Jung JS, Guggino WB and Agre P (1993) The mercury-sensitive residue at cysteine 189 in the CHIP28 water channel. *The Journal of biological chemistry* **268**(1):17-20.
- Reizer J, Reizer A and Saier MH, Jr. (1993) The MIP family of integral membrane channel proteins: sequence comparisons, evolutionary relationships, reconstructed pathway of evolution, and proposed functional differentiation of the two repeated halves of the proteins. *Critical reviews in biochemistry and molecular biology* **28**(3):235-257.
- Saparov SM, Kozono D, Rothe U, Agre P and Pohl P (2001) Water and ion permeation of aquaporin-1 in planar lipid bilayers. Major differences in structural determinants and stoichiometry. *J Biol Chem* **276**(34):31515-31520.
- Schwab A, Nechyporuk-Zloy V, Fabian A and Stock C (2007) Cells move when ions and water flow. *Pflug Arch Eur J Phy* **453**(4):421-432.

- Seeliger D, Zapater C, Krenc D, Haddoub R, Flitsch S, Beitz E, Cerda J and de Groot BL (2013) Discovery of novel human aquaporin-1 blockers. *ACS Chem Biol* **8**(1):249-256.
- Sogaard R and Zeuthen T (2008) Test of blockers of AQP1 water permeability by a high-resolution method: no effects of tetraethylammonium ions or acetazolamide. *Pflugers Arch* **456**(2):285-292.
- Sui H, Han B-G, Lee JK, Walian P and Jap BK (2001) Structural basis of water-specific transport through the AQP1 water channel. *Nature* **414**(6866):872-878.
- Trott O and Olson AJ (2010) AutoDock Vina: improving the speed and accuracy of docking with a new scoring function, efficient optimization, and multithreading. *J Comput Chem* **31**(2):455-461.
- Tsunoda SP, Wiesner B, Lorenz D, Rosenthal W and Pohl P (2004) Aquaporin-1, nothing but a water channel. *J Biol Chem* **279**(12):11364-11367.
- Yool AJ (2007) Functional domains of aquaporin-1: keys to physiology, and targets for drug discovery. *Curr Pharm Des* **13**(31):3212-3221.
- Yool AJ, Brown EA and Flynn GA (2009) Roles for novel pharmacological blockers of aquaporins in the treatment of brain oedema and cancer. *Clin Exp Pharmacol Physiol* **37**(4):403-409.
- Yool AJ and Campbell EM (2012) Structure, function and translational relevance of aquaporin dual water and ion channels. *Mol Aspects Med* **33**(5):443-561.
- Yool AJ, Morelle J, Cnops Y, Verbavatz JM, Campbell EM, Beckett EA, Booker GW, Flynn G and Devuyst O (2013) AqF026 is a pharmacologic agonist of the water channel aquaporin-1. *J Am Soc Nephrol* **24**(7):1045-1052.
- Yool AJ, Stamer WD and Regan JW (1996) Forskolin stimulation of water and cation permeability in aquaporin-1 water channels. *Science* **273**(5279):1216-1218.
- Yoshida T, Hojo S, Sekine S, Sawada S, Okumura T, Nagata T, Shimada Y and Tsukada K (2013) Expression of aquaporin-1 is a poor prognostic factor for stage II and III colon cancer. *Mol Clin Oncol* **1**(6):953-958.

- Yu J, Yool AJ, Schulten K and Tajkhorshid E (2006) Mechanism of gating and ion conductivity of a possible tetrameric pore in aquaporin-1. *Structure* **14**(9):1411-1423.
- Zhang H and Verkman AS (2015) Aquaporin-1 water permeability as a novel determinant of axonal regeneration in dorsal root ganglion neurons. *Exp Neurol* **265**:152-159.
- Zhang W, Zitron E, Homme M, Kihm L, Morath C, Scherer D, Hegge S, Thomas D, Schmitt CP, Zeier M, Katus H, Karle C and Schwenger V (2007) Aquaporin-1 channel function is positively regulated by protein kinase C. *J Biol Chem* **282**(29):20933-20940.

## Footnotes

MK and JVP are co-first authors.

This work was supported in part by the National Institutes of Health [Grant R01 GM059986]; and a 2015 pilot grant from The Institute for Photonics & Advanced Sensing, University of Adelaide.

## Figure Legends

**Figure 1.** Chemical structures of selected bumetanide derivatives and electrophysiology traces showing representative effects of AqB001, AqB006, AqB007, and AqB011 on the ionic conductance responses activated by bath application of CPT-cGMP, before and after 2 h incubation in saline with and without the AqB compounds. See Methods for details.

**Figure 2.** Trend plots showing the ionic conductance responses for individual oocytes measured prior to cGMP (initial), after the first cGMP application, after 2 h incubation in saline without cGMP containing DMSO (vehicle) or AqB agents, and after the second application of cGMP. Reversible cGMP-dependent activation of an ionic conductance in AQP1-expressing oocytes (A) was not seen in non-AQP1 control oocytes (B). Inhibition was seen after treatment with AqB007, and AqB011, but not with vehicle, AqB001, or AqB006.

**Figure 3.** Dose-dependent block of the AQP1 ionic conductance. (A) Compiled box plot data showing statistically significant block of the cGMP-activated ionic conductance in AQP1-expressing oocytes by AqB007 and AqB011, but not with vehicle, AqB001, or AqB006. See Methods for details. (B) Dose response curves showing percent block of the activated ionic conductance in AQP1 expressing oocytes and estimated  $IC_{50}$  values. *n* values for dose-response data (in order of increasing concentration) for AqB007 were 8, 4, 2, 8; and for AqB011 were 8, 2, 2, 3, 6, 4, 3.

**Figure 4.** Lack of effect of AqB compounds on AQP1 osmotic water permeability measured by optical swelling assays. (A) Mean oocyte volume, standardized as a percentage of the initial volume for each oocyte, as a function of time after introduction into 50% hypotonic saline, with and without 2 h pre-treatment with AqB compounds at 200  $\mu$ M, or vehicle (0.1% DMSO). (B) Compiled boxplot data showing the absence of any statistically significant differences between the first and second

swelling rates, measured before (S1) and after (S2) 2 h incubations in saline alone or saline with 200  $\mu$ M AqB compounds as indicated. See Methods for details.

**Figure 5.** In silico modeling of the energetically favored binding site for AqB011 in the center of the tetrameric channel of AQP1 (grey) at the intracellular side, bracketed by the gating loop D domains (green). The putative binding site suggests an interaction with two of the loop D domains from adjacent subunits. (A) is the full view of the tetramer, and (B) is a closer view slightly rotated to show proximity of the ligand to the conserved arginine residues in loop D.

**Figure 6.** Block of cell migration in AQP1-expressing HT29 but not SW480 cells treated with AqB011. (A) Illustrative diagram of the circular wound healing method, showing substantial closure of the wounded area in normal culture medium by 24 hours. (B) Compiled boxplot data from wound closure assays showing the dose-dependent inhibitory effects of AqB007 and AqB011, compared to DMSO and AqB006, on wound closure at 24 h in HT29 cell cultures. Migration of SW480 cells was not altered by AqB011.

**Supplemental Data.** Molecular modelling data in Protein Data Bank (pdb) format showing the compound AqB011 docked at the intracellular side of the tetrameric human AQP1 channel (PDB ID: 1FQY), and interacting with loop D domains of subunits surrounding the central pore.

**Table 1.** HT29 cell levels of cytotoxicity after 24 h incubation in culture medium with vehicle, AqB011 or HgCl<sub>2</sub>.

<b>Agent</b>	<b>Mean normalized cell viability (%) ± SEM<sup>§</sup></b>	<b>n value</b>	
[AqB011] μM			
0 (untreated)	100.0 ± 0.70	8	---
0 (0.1% DMSO)	103.9 ± 0.91	8	NS
1	104.0 ± 1.06	4	NS
5	102.3 ± 2.26	4	NS
10	110.6 ± 2.12	4	NS
20	114.0 ± 0.84	4	NS
40	111.8 ± 1.33	4	NS
80	102.4 ± 2.95	4	NS
HgCl <sub>2</sub> (100 μM)	16.2 ± 0.20	3	**

<sup>§</sup> Percent viability was standardized as a percentage of the untreated mean value, measured as changes in alamarBlue fluorescence signal intensity. See Methods for details.



Figure 1

vehicle

DMSO

AqB001

AqB006

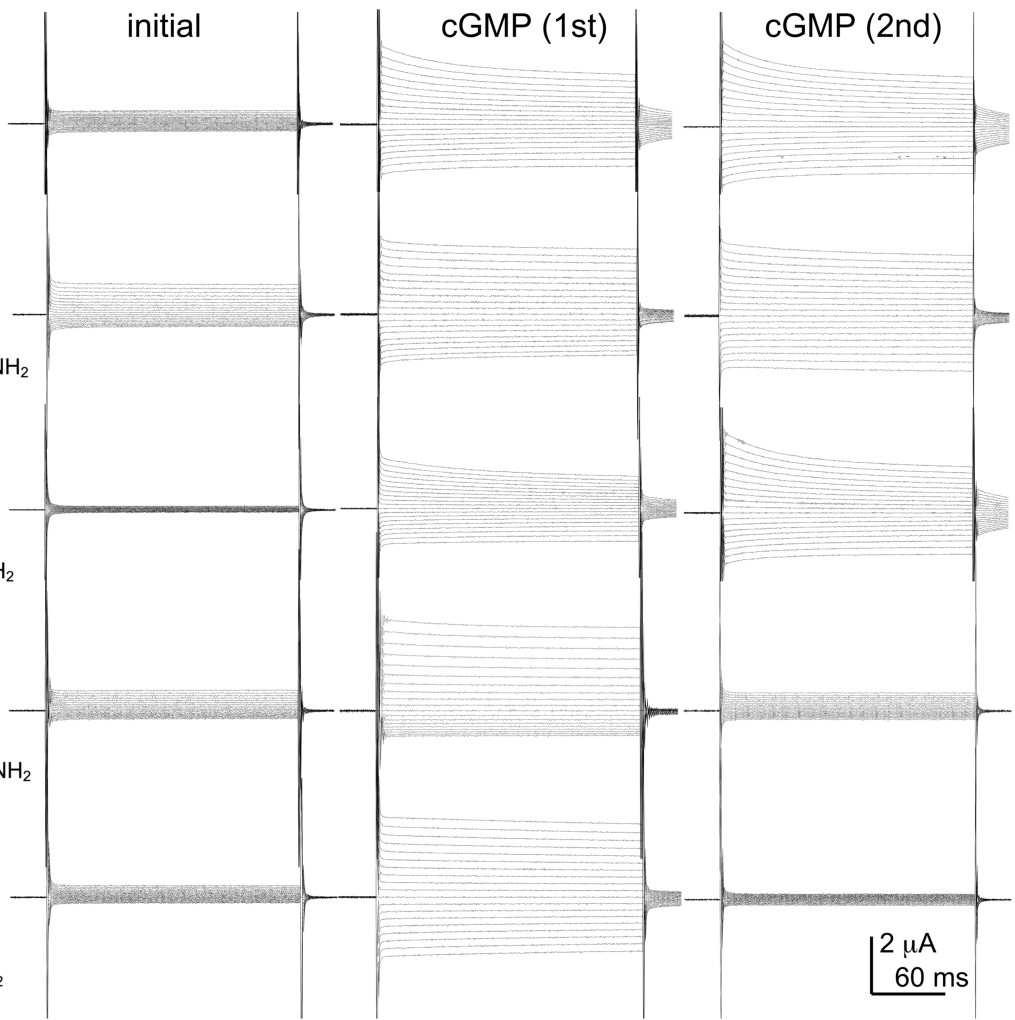
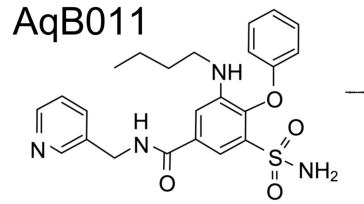
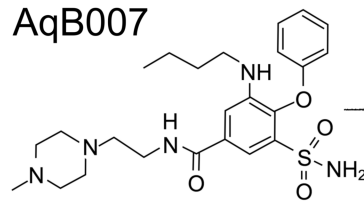
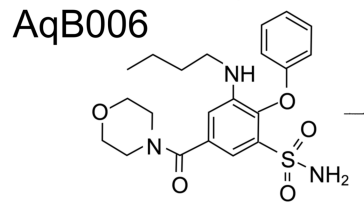
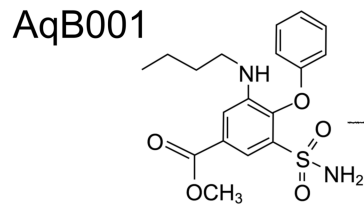
AqB007

AqB011

initial

cGMP (1st)

cGMP (2nd)



2  $\mu$ A  
60 ms

Figure 2

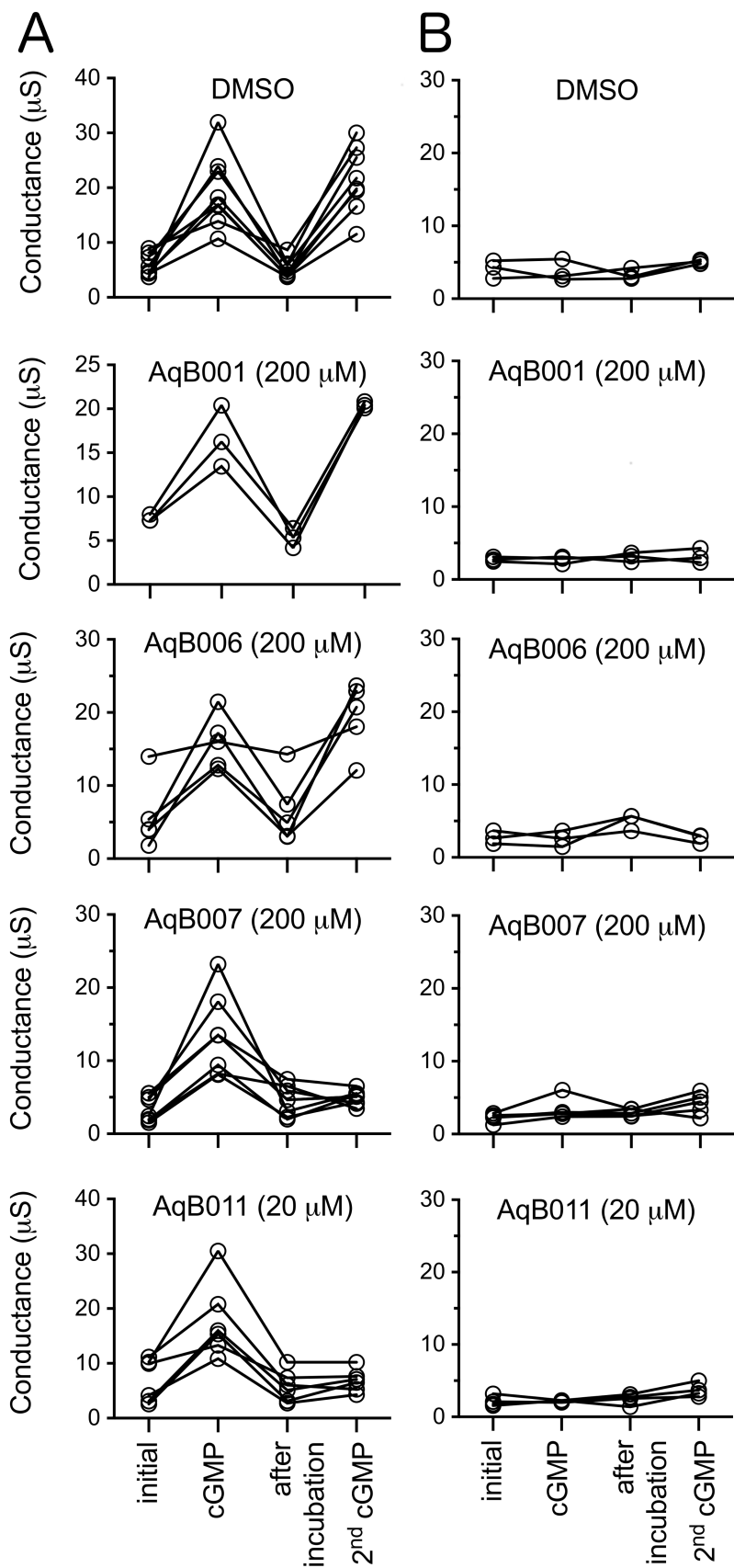
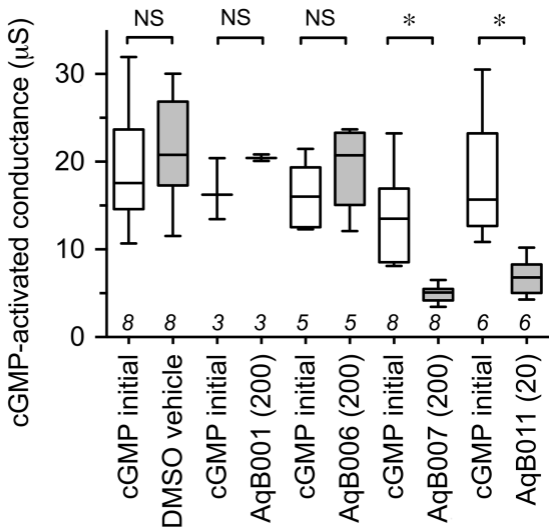


Figure 3

**A**



**B**

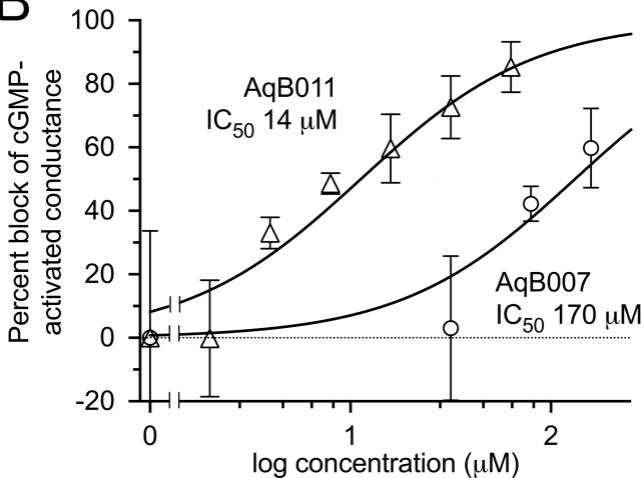


Figure 4

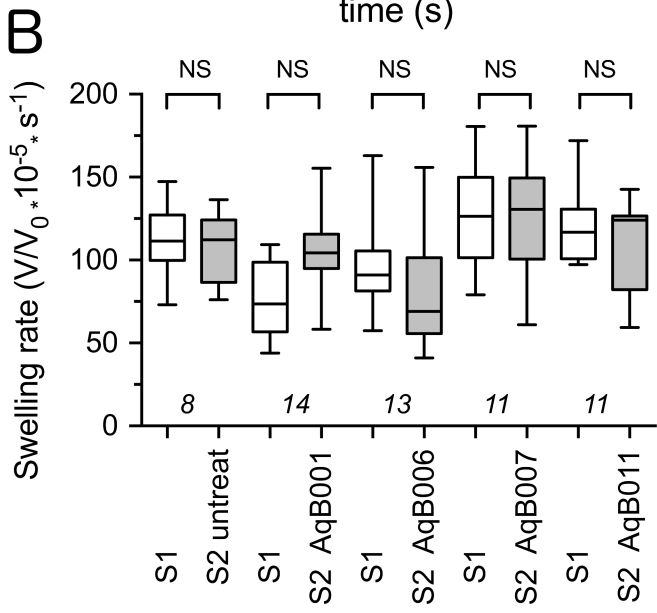
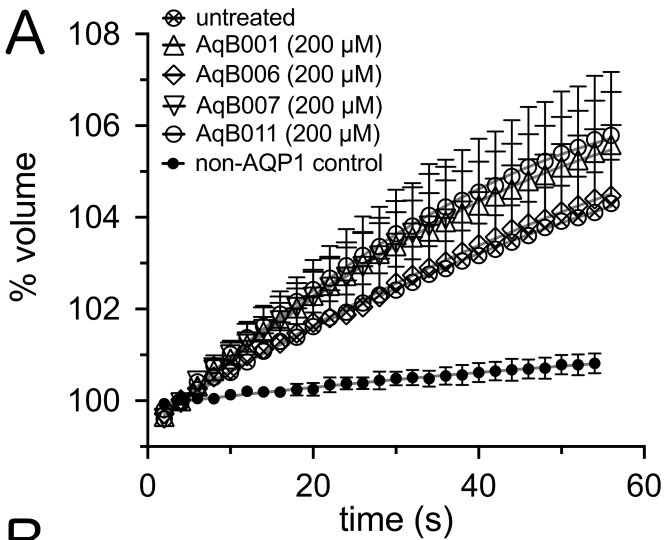
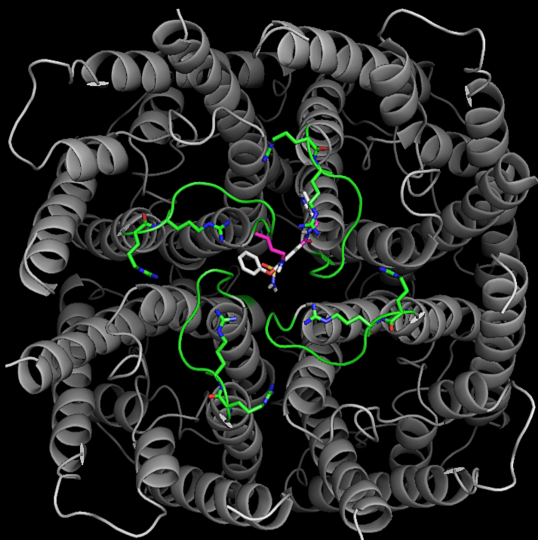


Figure 5

A



B

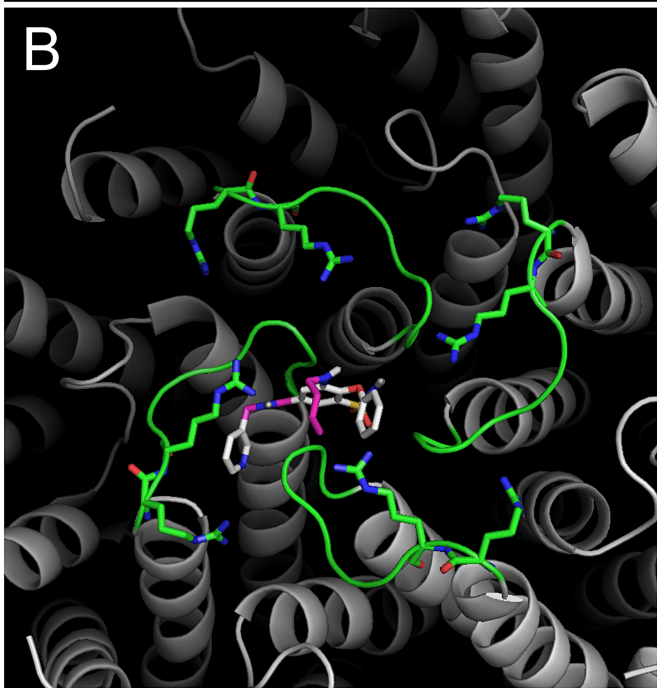


Figure 6

